Supporting materials to

« Optical detection of infectious SARS-CoV-2 virions by counting spikes»

Denis S. Kudryavtsev,[a,b] Vera A. Mozhaeva,[a] Igor A. Ivanov,[a] Andrey E. Siniavin,[a,c]
Alexey S. Kalmykov,[d] Anton S. Gritchenko,[d] Boris N. Khlebtsov,[e] Shao-Peng Wang,[f]
Bin Kang,[f] Victor I. Tsetlin,[a] Victor I. Balykin,[d] Pavel N. Melentiev[d,g,*]

[a.]Shemyakin-Ovchinnikov Institute of Bioorganic Chemistry of the RAS, Moscow 117997, Russia.

[b.]Department of Biology and General Genetics, I.M. Sechenov First Moscow State Medical University, 119048 Moscow, Russia

[c.]N.F. Gamaleya National Research Center for Epidemiology and Microbiology, Ivanovsky Institute of Virology, Ministry of Health, Moscow, Russia, 123098

[d.]Institute of Spectroscopy RAS, Moscow, Troitsk 108840, Russia.

[e.]Institute of Biochemistry and Physiology of Plants and Microorganisms, Saratov Scientific Centre of the Russian Academy of Sciences, Saratov, 410049, Russia

[f.]State Key Laboratory of Analytical Chemistry for Life Science and Collaborative Innovation Center of Chemistry for Life Sciences, School of Chemistry and Chemical Engineering, Nanjing University, Nanjing 210023, P. R. China.

[g.]Higher School of Economics, National Research University, Moscow, 101000, Russia

*Corresponding author's e-mail: melentiev@isan.troitsk.ru

Section 1. Synthesis of Core-Shell nanoparticles

Reagents. Dopamine hydrochloride (DA, H8502), Cetyltrimethylammonium bromide (CTAB, > 98.0%), cetyltrimethylammonium chloride (CTAC, 25% water solution), L-ascorbic acid (AA, >99,9), hydrochloric acid (HCl, 37 wt.% in water), tetraethyl orthosilicate (TEOS, 98%), thiolated polyethylene glycol (mPEG-SH, 99%), and sodium borohydride ($NaBH_4$, 99%) were purchased from Sigma-Aldrich. Cy7.5–amine was obtained from Lumiprobe. Hydrogen tetrachloroaurate trihydrate ($HAuCl4 \cdot 3H_2O$) and silver nitrate ($AgNO_3$, >99%) were purchased from Alfa Aesar. Ultrapure water obtained from a Milli-Q Integral 5 system was used in all experiments.

Synthesis of AuNRs. Au NRs with diameters of about 10-12 nm were synthesized by a seed-mediated growth method[1] with minor modifications concerning the concentrations of some reagents and reaction protocols. First, seed gold particles are prepared by adding aqueous sodium borohydride (10 mM, 0.6 ml) to a mixed aqueous solution of CTAB (0.1M, 10 ml) and $HAuCl_4$ (10 mM, 0.25 ml). For preparation of AuNRs with the aspect ratio of about 4, 1 ml of 4 mM $AgNO_3$, 2.5 ml of 10 M $HAuCl_4$, 0.5 ml of 80 mM AA, 0.5 ml of 1M HCl, and 0.5 ml of gold seed solutions are sequentially added to 50 ml of 0.1 M CTAB solution. The nanorods are allowed to grow overnight without stirring at 30 °C.

Coating with PDA shell containing Cy 7.5 molecules. First, the prepared nanorods were PEGilated using procedure described elsewhere.[2] After PEGilation AuNRs were dispersed in water in concentration of 300 µg/mL which correspond to number concentration of 45×10^{11} mL^{-1}. PDA shell were grown on the surface of

PEGilated nanorods. Tho this end 1 mL of AuNRs was mixed with 2 mL of water and 300μL of 100 mM Tris buffer (pH=8.5). Dopamine (DA) solutions at initial concentration 5 mg/mL were freshly prepared in water. Next, 100 μL of DA solution was quickly injected into the mixture and allowed to react for 3 h at the room temperature under continuous stirring (500 rpm). To initiate formation of Cy 7.5 embedded PDA shell 5 μL of Cy 7.5 amine solution in DMSO (1 mg/mL) were added to a batch with nanorods during shell growth process to get concentration of Cy 7.5 molecules in PDA shell equal to n=2.5×10^{18}cm^{-3}. The concentration was controlled in the extinction measurement of samples containing known concentration of Core-Shell nanostructures. The as-synthesized PDA coated nanorods with Cy7.5 was purified by repeated centrifugation at 12000 g for 15 min and finally resuspended in 3 mL of water.

Calculation of number of Cy 7.5 molecules in a shell of a single Core-Shell nanostructure. With the realized concentration of Cy 7.5 molecules n=2.5×10^{18}cm^{-3}, the average number of the molecules N in a shell of a single nanostructure can be estimated as $N = nV_{Shell} \approx 2.5 \times 10^{18} cm^{-3} \times 3.85 \times 10^{5}\, nm^3 = 9.6 \times 10^{23} cm^{-3} \times 10^{-21} cm^3 \approx 10^3$ **molecules**. Here V_{Shell} is a volume of the Shell of a nanostructure, calculated with the use of typical geometrical parameters of a Core-Shell nanostructure obtained from corresponding electron microscopy images (Fig. 3a of the main text): $V_{Shell} = \frac{4\pi}{3}(60 \times 40 \times 40 - 40 \times 10 \times 10)\, nm^3 = 3.85 \times 10^{5}\, nm^3$.

Section 2. Labeling of Core-Shell nanostructures

Anti-RBD monoclonal antibody was generated as described previously.[3] PDA coating of Core-Shell nanostructures was prepared in the presence of ethylenediamine (1 mole %) to achieve incorporation of free amino groups, which later were used to covalently cross-link antibodies. To attach antibodies covalently to amino groups in PDA coating of Core-Shell NPs, the following procedure was used: freshly prepared Core-Shell nanostructures were suspended in 50 mM $NaHCO_3$, then 50 mM solution of succinic anhydride in acetonitrile was added. The resulting mixture was shaken for 8 h to allow amino groups react with succinic anhydride. Then, succinyl-nanoparticles were centrifuged, washed twice with 50% acetonitrile, then re-suspended in the activation buffer (50 mM MES pH 5.8 in 50% acetonitrile). Sulfo-N-hydroxysuccinimde (sulfo-NHS, Sigma) and 1-Ethyl-3-(3-dimethylaminopropyl)carbodiimide (EDC, Sigma) were added to the suspension of Core-Shell nanostructures to the final concentration 10 mM. The mixture was shaken for 30 min, then centrifuged and 50 μL of the RBD protein solution (0.5 g/L) in PBS was added immediately to the precipitate of Core-Shell nanostructures with NHS-activated PDA coating. The resulting suspension was allowed to shake for 8 h at +4 C, then centrifuged (sample of un-bound protein solution was collected at this stage), washed with 25 mM ethanolamine in PBS, followed by PBS washes. The resulting Core-Shell nanostructures can be stored in PBS at +4 C for at least two months.

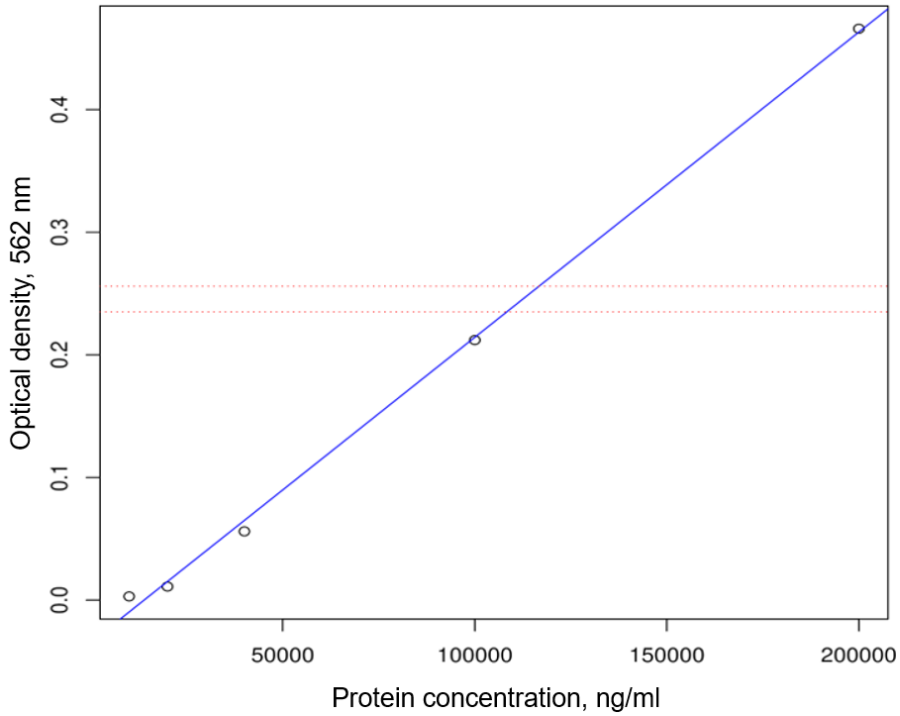

Figure S1. Unbound protein concentration measured after Core-Chell nanostructures centrifugation corresponds to 112 ± 6 μg/mL. The red dotted horizontal lines show the results of two independent measurements of the optical density of unbound antibody concentration after labeling of Core-Shell nanostructures.

Un-bound protein solution concentration was measured using microBCA kit (Thermo Scientific) according to manufacturer recommendations. A 50 μL of sample solution was collected by centrifugation and added to microBCA main reagent. Calibration curve (circles and blue line) is depicted on Fig. S1. Measured optical density (OD) at 562 nm is shown by dotted red horizontal lines. Thus un-bound protein concentration was measured to be 112 ± 6 μg/mL. In our experimental setup dry Core-Shell nanostructures occupy approximately 10% of the coupling reaction volume. According to measurements of unbound protein, 5 μL of nanoparticles absorbed about 20 ng of protein, which corresponds to 6×10^{13} molecules (0.1 mole) per 3×10^{13} nanoparticles. Thus at least two IgG antibody molecules are bound to each nanoparticle on average.

Section 3. Distribution of Core-Shell nanostructures on a substrate surface after the sample preparation procedure

An important point of the developed sample preparation protocol is distinguishing of Core-Shell nanostructures bound to the coronavirus particle from the unbound Core-Shell nanostructures. To achieve this goal, the coffee ring effect,[4] which is inherent to mesoscopic particles when the droplet dries during sample preparation, is used. When the droplet dries, the Core-Shell nanostructures in the solution are pushed out from the interior of the droplet towards the edges by a flow. At the edge of the droplet, the Core-Shell nanostructures are squeezed between the liquid surface and the glass substrate, accumulate and form large agglomerates. Figure S2 shows the dark-field optical image of the dried sample and SEM images of the central part and the edge of the dried droplet. It can be seen that the unbound Core-Shell nanostructures are mainly concentrated at the edge of the analyzed sample during the drying process. Thus, the density of Core-Shell nanostructures in the central part of the droplet is orders of magnitude lower than near the edge. Another important consequence of the coffee ring effect, which mainly affects smaller particles,[5] is that no large aggregates of

Core-Shell nanostructures are found in the central part of the dried droplet. As will be shown below, the distribution of Core-Shell nanostructures on the substrate realized in the developed sample preparation protocol thus creates ideal conditions for the detection of labeled viral or pseudoviral particles in the central part of the dried droplet, where the concentration of Core-Shell nanostructures is negligible. Due to the functionalizing layer on the substrate surface, the labeled viral and pseudoviral particles are chemically bound to the substrate when the droplets are dried, while the Core-Shell nanostructures move freely in the droplet.

The particles that appear on the surface of the substrate when the droplet dries are subject to the forces of the liquid flow and the forces of interaction with the surface (gravity and Archimedes' force can be neglected due to the small size of the particles). The force from the fluid flow can be described as the drag force $F_{flow} \propto R^2$. The flow acts in the direction along the surface. The forces of interaction of particles with a surface can be divided into electrostatic and van der Waals forces. In this case, the role of the van der Waals forces increases significantly with decreasing particle size and exceeds the contribution of the electrostatic forces.[6] The van der Waals forces are proportional to the contact area (the area on which the particle comes into contact with the surface). In this case, the contact areas are almost the same for particles with different diameters. These forces generate friction between the particles and the surface: $F_{VdW} \propto S_{contact} \sim const$. As the size of the agglomerate increases, the force on the flow side increases faster than the van der Waals forces, so that large particles are washed away to the edge as the droplet dries. Such large particles can be detected as false positives during detection, but the number of such particles near the center of the sample is small. Only small number of single unbound Core-Shell particles can be found in the central part (Figure S2, upper right SEM image).

The SEM image of the area inside the dried droplet (bottom right) shows the particles bound to the surface. The interpretation of the detected fluorescence signal, whether it originates from viral particles or from unbound Core-Shell nanostructures, is thus unambiguous in the central part of the dried droplet due to two factors: (1) the binding of the viral particles to the surface of the substrate, (2) a large number of Core-Shell nanostructures bound to a single SARS-CoV-2 virus (more than 40 for virulent viruses), and (3) the absence of a large number of unbound Core-Shell nanostructures in the central part of the dried droplet (see specific numbers below).

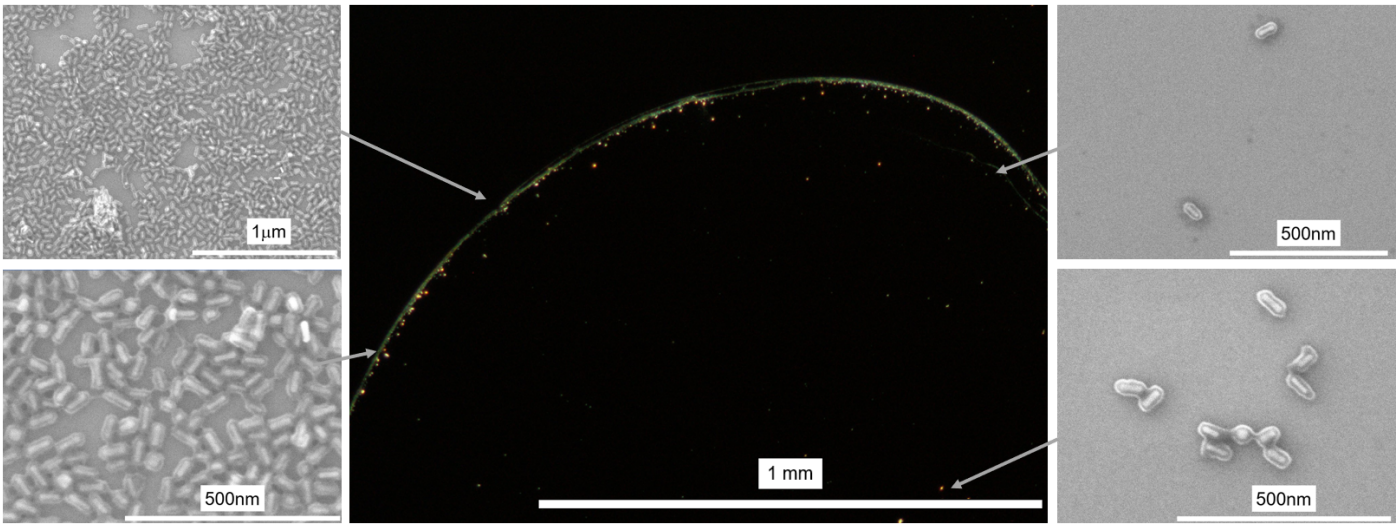

Figure S2. Microscopy of a dried droplet after sample preparation protocol of a sample without coronavirus particles and only with Core-Shell nanostructures with antibodies: (middle image) dark-field light microscopy of a sample showing the concentration of Core-Shell nanostructures near the edge of the droplet during drying (coffee ring) and a

small amount of the nanostructures in the center of the droplet, (images in the left and right columns) electronic images of the sample near the edge (shown on the left) and in the center (shown on the right) of the dried droplet.

Section 4. Fluorescent detection of a single Core-Shell nanostructures

For the developed protocol for counting spike proteins on the lipid surface of the SARS-CoV-2 virus, it is crucial to recognize a single Core-Shell nanostructure with sufficient accuracy and to have means to count a number of Core-Shell nanostructures of a diffraction-limited light source consisting of an aggregate of closely arranged Core-Shell nanostructures. The developed method is based on the measurement of photon flux emitted from a diffraction-limited light source and recorded in fluorescence microscopy.

In a first step, we measured the photon flux from a single Core-Shell nanostructure. Measuring the fluorescence of a sample containing a dried droplet with a Core-Shell nanostructure cannot be helpful for this purpose, as there are no ways to control the number of Core-Shell nanostructures, which form a single diffraction-limited light source due to the fluorescence of Core-Shell nanostructures under laser excitation (see Figure S2, which shows closely spaced Core-Shell nanostructures even in the central part of the dried droplet, whose mean distance is much smaller compared to the wavelength of fluorescence emission). For this purpose, we used a non-evaporated droplet with Core-Shell nanostructures that are constantly moving in the droplet due to Brownian motion and recorded their fluorescence emission, which helps us to monitor the motion. Our measurements have shown that the Core-Shell nanostructures in such an arrangement can be easily monitored and unambiguously determined (see Figure S3). Figure S3 shows a fluorescence microscopy image of 7 individual Core-Shell nanostructures. The signal of five of the nanostructures is almost the same and about 1.8 times higher than the signal of the other three Core-Shell nanostructures. The detailed analysis of Figure S3 shows that the difference is due to the fact that the five Core-Shell nanostructures are located in the sample plane of the ideal optical microscopy, while the other three Core-Shell nanostructures are slightly out-of-plane - the diameter of the light spots of the out-of-plane Core-Shell nanostructures is about 30% larger than the diameter of the light spots of Core-Shell nanostructures located in the ideal sample plane. Figure S3 thus shows the fluorescence microscopy of individual Core-Shell nanostructures and helps to determine an important parameter – the photon flux of an individual Core-Shell nanostructure.

Using the standard protocol for calibrating the optical sensor[7] and summing up all pixels of the CCD camera showing a diffraction-limited image of a single Core-Shell nanostructure, we obtain a value of $P_1=7\times10^3$ photons/s photon flux from a single Core-Shell nanostructure. We used this value to count the number N of Core-Shell nanostructures in a registered diffraction-limited light spot in the optical detection of coronavirus particles – the measured photon flux is $N\times P_1$ because, unlike fluorescent molecules, the fluorescence of Core-Shell nanostructures does not depend on their concentration. This is a rather trivial consequence, since most of the fluorescence comes from Cy 7.5 molecules located near the Au nanostructure, in the so-called plasmonic hotspots, which are covered by an arbitrarily thick polydopamine layer that prevents interference of these molecules with molecules in another Core-Shell nanostructure.

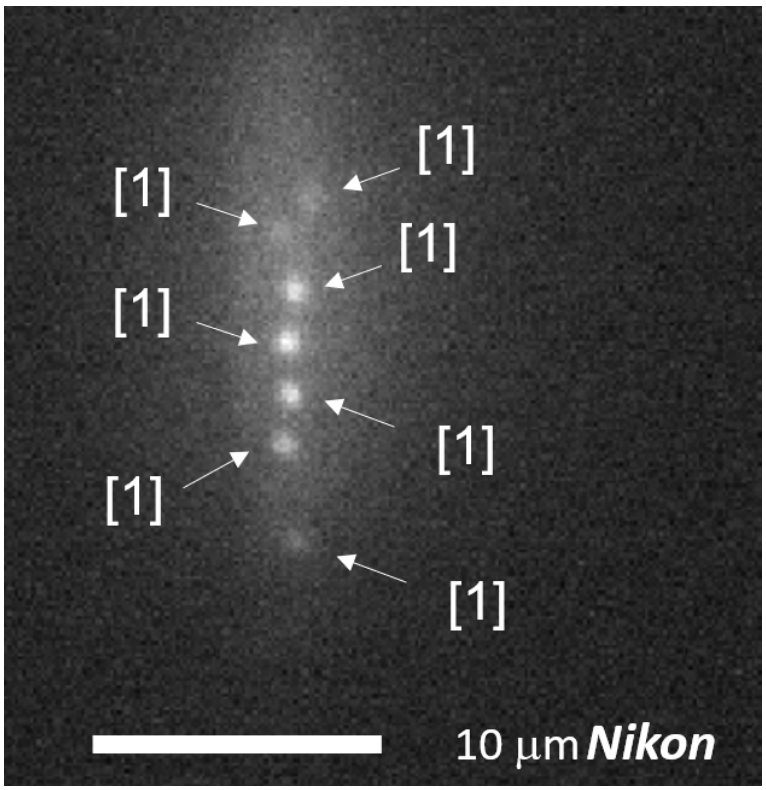

Figure S3. Fluorescence image of a sample for calibration of fluorescent flux from a single Core-Shell nanostructure. The numbers in square brackets indicate the number of measured Core-Shell nanostructures forming a bright light spot indicated by the corresponding arrow.

Figure S4 shows the results of measurements on a sample droplet without virus particles: fluorescence image of the central part of the droplet under 780-nm laser light excitation, showing the detection of the counted number of Core-Shell nanostructures forming localized light sources. The numbers in square brackets indicate the number of measured Core-Shell nanostructures forming a bright light spot indicated by the corresponding arrow. The numbers were determined using a method described above in which the photon flux from detected diffraction-limited point-like light sources, seen as white dots in the figure, was analyzed. As can be seen from the figure, there are no large aggregates of Core-Shell nanostructures in the central part of the dried droplet, which covers about 40% of its surface.

Figure S5 shows the probability distribution measured over 12 samples (with more than 100 diffraction limited spots analyzed) for the detection of agglomerates of Core-Shell nanostructures in a central region of a dried drop covering approximately 85% of the surface area of the dried drop (see Figure S4 for an example of the measurement for one sample). The navy blue line shows the result of the chi-square approximation. As can be seen from the figure, the Core-Shell nanostructures in the developed protocol without virus particles do not form aggregates with more than 7 nanostructures. The approximated probability distribution curve shows that the possibility of the formation of aggregates with more than 40 Core-Shell nanostructures is negligible and much lower than 0.1%. This is a very important result that shows that the probability of a false positive result in the detection of viruses is quite low. In the developed approach, about 85% of the surface of the dried droplet was examined for the presence of large aggregates of Core-Shell nanostructures. The other part of the droplet is located near the edges of the droplet and may contain large aggregates. It is possible that the virus particles are located exactly in this area near the edge of the droplet and therefore cannot be detected with the developed protocol. Therefore, the probability of false negative results can be estimated at 15 %. This value is quite acceptable for the practical implementation of the developed method, as the known and widely used methods for the detection of coronaviruses have practically the same false negative detection probability.[8]

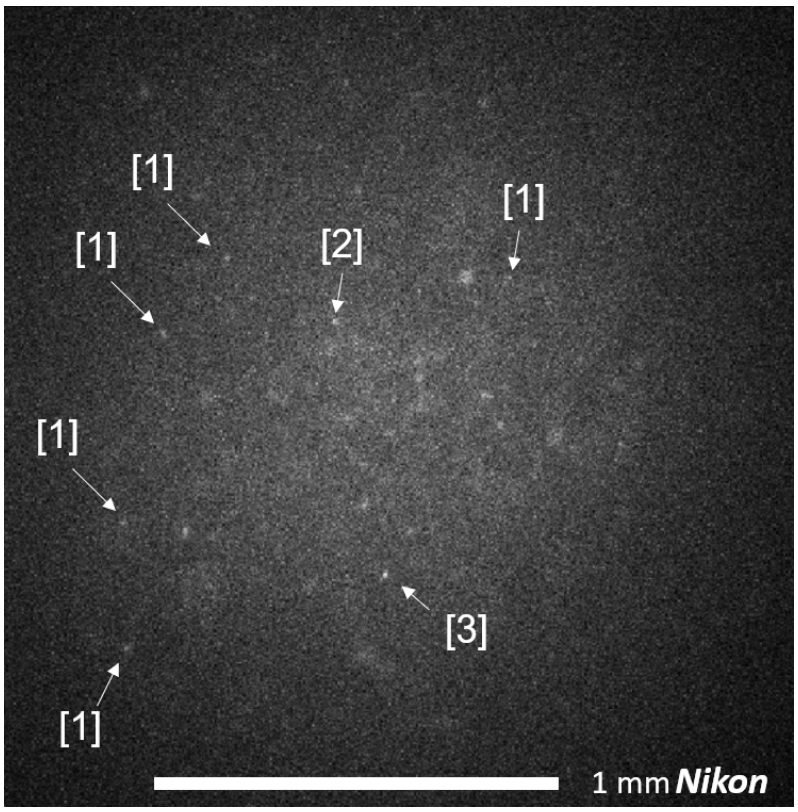

Figure S4. Sample droplet without virus particles: fluorescence image of the central part of the droplet under 780-nm laser light excitation, showing the detection of the counted number of Core-Shell nanostructures forming localized light sources. The numbers in square brackets indicate the number of measured Core-Shell nanostructures forming a bright light spot indicated by the corresponding arrow.

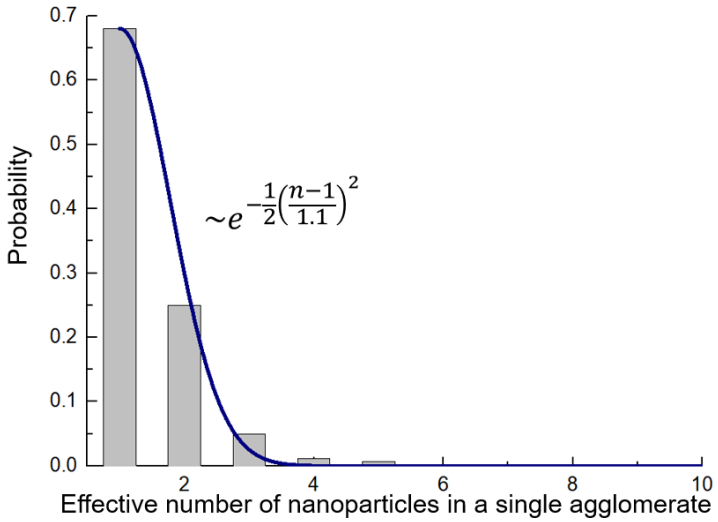

Figure S5. Probability distribution measured over 12 samples for the detection of agglomerates of Core-Shell nanostructures in a central region of a dried droplet covering approximately 85% of the surface of the dried droplet (see Figure S4 for an example of the measurement for one sample). The navyblue line shows the result of the chi-squared approximation.

References

(1) Nikoobakht, B.; El-Sayed, M. A. Preparation and Growth Mechanism of Gold Nanorods (NRs)

Using Seed-Mediated Growth Method. *Chemistry of Materials* **2003**, *15* (10), 1957–1962.

(2) Niidome, T.; Yamagata, M.; Okamoto, Y.; Akiyama, Y.; Takahashi, H.; Kawano, T.; Katayama, Y.; Niidome, Y. PEG-Modified Gold Nanorods with a Stealth Character for in Vivo Applications. *Journal of Controlled Release* **2006**, *114* (3), 343–347.

(3) Antipova, N. V; Larionova, T. D.; Siniavin, A. E.; Nikiforova, M. A.; Gushchin, V. A.; Babichenko, I. I.; Volkov, A. V; Shakhparonov, M. I.; Pavlyukov, M. S. Establishment of Murine Hybridoma Cells Producing Antibodies against Spike Protein of SARS-CoV-2. *International Journal of Molecular Sciences Article* **2020**, *21* (23), 9167.

(4) Jeong, H.; van Tiem, J.; Gianchandani, Y. B.; Park, J. NANO-PARTICLE SEPARATION USING MARANGONI FLOW IN EVAPORATING DROPLETS. In *Solid-State Sensors, Actuators and Microsystems Workshop*; South Carolina, 2014.

(5) Wong, T. S.; Chen, T. H.; Shen, X.; Ho, C. M. Nanochromatography Driven by the Coffee Ring Effect. *Analytical Chemistry* **2011**, *83* (6), 1871–1873.

(6) Rajupet, S.; Riet, A. A.; Chen, Q.; Sow, M.; Lacks, D. J. Relative Importance of Electrostatic and van Der Waals Forces in Particle Adhesion to Rough Conducting Surfaces. *Physical Review E* **2021**, *103* (4), 042906.

(7) Gritchenko, A.; Eremchev, Iy.; Naumov, A.; Melentiev, P.; Balykin, V. Single Quantum Emitters Detection with Amateur CCD: Comparison to a Scientific-Grade Camera. *JOLT* **2021**.

(8) Pecoraro, V.; Negro, A.; Pirotti, T.; Trenti, T. Estimate False-negative RT-PCR Rates for SARS-CoV-2. A Systematic Review and Meta-analysis. *European journal of clinical investigation* **2022**, *52* (2), e13706.